Asian Journal of Water, Environment and Pollution. Vol. 22, No. 6 (2025), pp. 221-242.
doi: 10.36922/AJWEP025350269

ORIGINAL RESEARCH ARTICLE

Spatiotemporal dynamics of fractional vegetation cover and its relationship with climatic factors in the Yarkand River Basin

Guoqiang Qin[1,2]*, Kai Yuan[1,2], Guoliang Ding[3], Qiang Guo[1,2], and Runbo Wang[1,2]

[1]Department of Hydraulic Engineering Management, College of Hydraulic and Civil Engineering, Xinjiang Agricultural University, Urumqi, Xinjiang, China
[2]Xinjiang Key Laboratory of Water Engineering Safety and Disaster Mitigation, College of Hydraulic and Civil Engineering, Xinjiang Agricultural University, Urumqi, Xinjiang, China
[3]Department of Environmental Protection Engineering, XPCC Surveying and Designing Institute Group Co., Ltd., Urumqi, Xinjiang, China
***Corresponding author:** Guoqiang Qin (qinguoqiang1988@163.com)

Received: August 25, 2025; 1st revised: September 16, 2025; 2nd revised: September 23, 2025; Accepted: September 28, 2025; Published online: October 24, 2025

Abstract: The Yarkand River Basin, an ecologically fragile zone in arid northwest China, is critical for regional ecological management due to its sensitivity to environmental changes. This study examines the spatiotemporal dynamics of fractional vegetation cover (FVC) from 2000 to 2023 and its correlation with climatic factors, using the moderate resolution imaging spectroradiometer (MODIS) normalized difference vegetation index data and climate observations (temperature and precipitation). FVC was estimated using the pixel dichotomy method, with Sen+Mann–Kendall trend analyses, and Pearson correlation was applied to assess temporal trends and climate-vegetation relationships. MODIS land use data were reclassified to evaluate FVC variations across forestland, grassland, farmland, bare land, and other ecological types. Results revealed significant spatiotemporal heterogeneity in FVC. Spatially, Yecheng County exhibited higher FVC than Bachu County, driven by favorable topography. Temporally, FVC showed a significant upward trend post-2000, particularly in grasslands and croplands, stabilizing between 2010 and 2023. Climate analysis indicated divergent responses: farmland and forest FVC were negatively correlated with temperature (ranging from 8°C to over 9°C). In contrast, grassland and forest FVC were positively associated with precipitation (increasing by ~14 mm). A 1–2-month lag effect was observed in precipitation's impact on FVC. The Hurst index suggested a sustained FVC growth in most regions. These findings highlight the role of climate change in driving FVC dynamics, providing a scientific basis for ecological conservation and sustainable water resource management in arid regions.

Keywords: Yarkand River Basin; Fractional vegetation cover; Land use types; Climatic factors; Ecological management

1. Introduction

Fractional vegetation cover (FVC), a standardized ecological indicator, serves as a critical measure for quantifying the extent of surface vegetation, playing an indispensable role in ecosystem material cycles, energy balance, and regional climate regulation.[1] As a key parameter reflecting vegetation growth status, FVC not only visually delineates spatial distribution patterns of vegetation but also provides essential data for assessing ecosystem service functions, such as carbon sequestration and soil conservation. Against the backdrop of global climate change, climatic factors, such as temperature and precipitation, exert a significant influence on FVC, with arid and semi-arid regions displaying heightened sensitivity to these variations.[2,3] The fragile ecosystems in these areas amplify the ecological consequences, where even subtle FVC fluctuations can trigger cascading effects on processes, such as carbon cycling and surface albedo, ultimately influencing regional and global climate systems. This underscores the urgency of monitoring and understanding FVC dynamics to support sustainable environmental management.

Remote sensing technology has emerged as a cornerstone for studying FVC, leveraging its high spatiotemporal resolution and extensive coverage to monitor vegetation dynamics effectively.[4] Core indicators, such as the normalized difference vegetation index (NDVI) and its derivative, FVC, derived from datasets including the moderate resolution imaging spectroradiometer (MODIS) and Landsat, have yielded significant insights across various river basins.[5] Common methodologies include the coefficient of variation (CV) to assess temporal stability, Sen+Mann–Kendall trend analysis for detecting long-term trends, and Pearson correlation analysis to explore climatic relationships. These approaches, widely validated in arid region studies, provide a robust framework for analyzing FVC spatiotemporal patterns. Building on this foundation, this study employs CV, Sen+Mann–Kendall trend analysis, and Pearson correlation to investigate FVC dynamics in the Yarkand River Basin, thereby enhancing the precision and scope of FVC research.

The Yarkand River Basin, located in the northern Tarim Basin of Xinjiang, China, is a core arid region characterized by a fragile ecological environment. Changes in its FVC significantly impact regional balance in ecology and are intricately linked to several key factors, such as water resources. The water resources not only supply the necessary moisture for vegetation growth but also influence the soil environment that sustains such growth, indirectly affecting vegetation.[6] Other key factors include land use and human activities.[7] As an integral part of the Tarim River Basin, the vegetation dynamics of the Yarkand River Basin are shaped by complex terrain—encompassing alpine glaciers, oasis agricultural zones, and desert ecosystems—and diverse vegetation types, including grasslands, shrubs, croplands, and sparse vegetation.[8] Since 2000, global warming has driven temperature increases and altered precipitation patterns, profoundly affecting vegetation growth and distribution.[9] Previous studies have highlighted that FVC in arid areas typically correlates positively with precipitation, while rising temperatures may inhibit growth through enhanced evapotranspiration.[10,11] Human interventions, such as agricultural irrigation, urbanization, and ecological restoration projects, further influence these dynamics.[12,13] However, existing research, often limited to shorter time scales or single vegetation types, lacks a comprehensive analysis of long-term FVC spatiotemporal variations, county-level differences, and the response mechanisms of diverse vegetation types from 2000 to 2023.[14,15] This gap highlights the need for an in-depth investigation into these aspects.

This study, based on remote sensing data from 2000 to 2023, employs CV, Sen+Mann–Kendall trend analysis, and Pearson correlation to systematically explore the spatiotemporal variation characteristics of FVC in the Yarkand River Basin and its relationship with temperature and precipitation. This study utilizes the latest MODIS NDVI data (MOD13Q1 V6) spanning the extended period from 2000 to 2023 to capture long-term FVC trends and analyzes FVC spatial heterogeneity at the county and land use type scales. The significance of this work lies in: (i) enhancing the understanding of vegetation dynamics and climate response mechanisms in the Yarkand River Basin, offering a reference for regional ecosystem research; (ii) providing a scientific foundation for ecological protection and climate adaptation management in arid regions; and (iii) supporting data-driven water resource management and sustainable development initiatives.

2. Materials and methods

2.1. Overview of the study area

The Yarkand River Basin (36°02'–41°22' north, 75°14'–81°47' east), as shown in Figure 1, is located in the northern part of the Tarim Basin in Xinjiang, China, with a total area of approximately 110,000 km^2, accounting for about 10.7% of the area of the Tarim

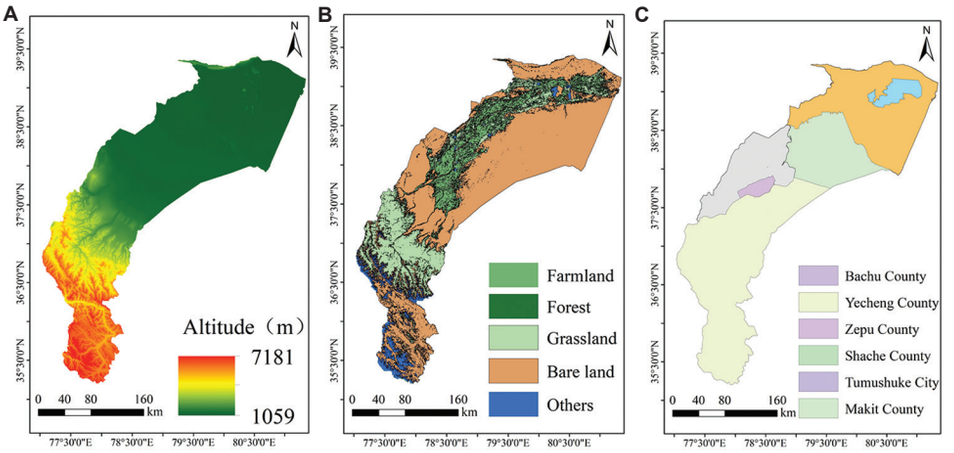

Figure 1. Schematic representation of the Yarkand River Basin. (A) Elevation. (B) Land use types. (C) Administrative division.

Basin.[16] The terrain of this basin is complex, extending from northwest to southeast, covering the alpine glaciers of the Pamir Plateau, the oasis agricultural areas, and the desert area on the edge of the Taklimakan Desert. More than 60% of the area is mountainous and plateau, with an altitude generally above 1,500 m, and the highest peak reaching above 7,000 m.[17] The Yarkand River Basin has a typical continental arid climate. Winters are cold and dry, and summers are short and hot. The average annual temperature ranges from 5 to 12°C. The annual precipitation varies from 300 mm in high mountain areas to <50 mm in lowland oases, showing significant spatial heterogeneity.[18] This climatic condition supports diverse land use types, including bare land, grassland, shrub, farmland, and sparse vegetation. Bare land and sparse vegetation are mainly distributed in arid desert areas, grasslands and shrubs are concentrated in high mountains and the edges of oases, and farmlands are primarily distributed in the irrigated oasis areas along the Yarkand River.[19] These geomorphic and climatic characteristics make the Yarkand River Basin a vital area for studying the relationship between FVC and climate change.[20]

2.2. Remote sensing data sources and processing

2.2.1. Land use type data

In this study, MODIS MCD12Q1 products (2000–2023) were adopted, and land use types in the Yarkand River Basin were extracted and reclassified using the Google Earth Engine (GEE) platform. Based on the 17-category classification system of the International Geosphere-Biosphere Project, the original data were integrated into five categories: forest land, grassland, bare land, farmland, and others, to reflect the ecological functions of the various vegetation types.[21] By leveraging the computing power of the GEE platform, annual land use data from 2000 to 2023 were generated, and GeoTIFF format images were exported using the mode synthesis method, providing high-resolution data support for analyzing the relationship between FVC and climate.[22] This classification and synthesis method provided a reliable data basis for investigating the correlation between vegetation dynamics and climatic factors in the Yarkand River Basin.

2.2.2. NDVI data

This study utilized the MODIS (MOD13Q1) NDVI dataset from the National Aeronautics and Space Administration Earth Observing System/MODIS, with a spatial resolution of 250 m and a time range of 2000–2023. To ensure data accuracy, the image was first processed by cloud, shadow, and water mask processing, and only the NDVI band was retained. Subsequently, the maximum value synthesis method was employed to generate the annual maximum NDVI image, which reflects the optimal state of vegetation growth in the Yarkand River Basin. Through a 5% and 95% quantile analysis, the high and low value ranges of regional NDVI were extracted to characterize the spatiotemporal dynamics of FVC. Similar to the study conducted by Kaur *et al.*,[23] we utilized NDVI thresholding to classify vegetation into several categories, such as sparse, moderate, and dense, adjusting thresholds based on regional vegetation health. The processed NDVI data provide high-resolution support for analyzing the relationship between FVC and temperature and precipitation. In response to concerns about potential errors from relying solely on remote sensing data without

ground validation, we conducted field measurements at selected sites (e.g., Yecheng, Shache, and Zepu counties) using a handheld NDVI device (GreenSeeker RT200, Trimble Inc., United States of America), which showed good agreement between remote sensing data and ground-measured NDVI values, with a correlation coefficient (R^2) exceeding 0.85. This validation enhances the reliability of the MODIS NDVI dataset for ecological analysis in the study area.

2.2.3. Meteorological data

In this study, the China Meteorological Administration (CMA) daily dataset was utilized to obtain temperature and precipitation data for the Yarkand River Basin from 2000 to 2023. Data were collected from approximately 2,400 meteorological stations across China using the Vaisala HMP155A (Vaisala Oyj, Finland) temperature and humidity sensor for temperature measurements, and the Tipping Bucket Rain Gauge RG13-H (Vaisala Oyj, Finland) for precipitation measurements, with a spatial resolution of 1 km. To align with the 250 m resolution of the MODIS NDVI data used for FVC analysis, the CMA data were resampled using ArcGIS software (ArcGIS 10.8, ESRI, United States of America). By overlaying land use type maps (forest land, grassland, bare land, farmland, and others), we generated annual average temperatures and total precipitation for each land type. In addition, by integrating the administrative boundaries of counties and cities, we extracted annual average temperatures and precipitation for each administrative unit to assess the spatial heterogeneity of the regional climate. The annual temperature and precipitation data for the entire region were calculated as average values to reveal the overall trend of climate change. A public access link for the CMA dataset is available at http://data.cma.cn.

2.3. Research methodology

2.3.1. Pixel dichotomy

In this study, the FVC of the Yarkand River Basin for 2000–2023 was estimated using the pixel dichotomy method, which decomposes the image spectra into vegetative and non-vegetative components to calculate the FVC (Equation I).

$$FVC = \frac{NDVI - NDVI_{min}}{NDVI_{max} - NDVI_{min}} \quad \text{(I)}$$

Where NDVI is the image element NDVI value, $NDVI_{max}$ and $NDVI_{min}$ are the 95% and 5% confidence values of the regional NDVI gray scale distribution, reflecting pure vegetation and bare soil characteristics, respectively.[24] Combined with the dynamic adjustment thresholds for land use types (woodland, grassland, bare land, farmland, etc.), the FVC was categorized into five levels: low coverage ($0 \leq FVC < 0.2$), medium-low coverage ($0.2 \leq FVC < 0.4$), medium coverage ($0.4 \leq FVC < 0.6$), medium-high coverage ($0.6 \leq FVC < 0.8$), and high coverage ($0.8 \leq FVC \leq 1$).[25]

2.3.2. CV

In this study, the CV was used to quantify the interannual fluctuations of FVC in the Yarkand River Basin from 2000 to 2023, assessing vegetation stability (Equation II).

$$CV_{FVC} = \frac{\sigma_{FVC}}{\overline{FVC}} \quad \text{(II)}$$

Where σ_{FVC} is the standard deviation, and $\overline{FVC}$ is the mean FVC over the 24 years. A smaller CV_{FVC} indicates lower fluctuation. Combining land use types (forest land, grassland, bare land, farmland, etc.) and county/city classifications, spatial differences in FVC fluctuation were analyzed. FVC fluctuation was categorized into five levels: low fluctuation change ($CV_{FVC} \leq 0.1$), lower fluctuation change ($0.1 < CV_{FVC} \leq 0.15$), medium fluctuation change ($0.15 < CV_{FVC} \leq 0.2$), higher fluctuation change ($0.2 < CV_{FVC} \leq 0.3$), and high fluctuation change ($CV_{FVC} > 0.3$).[26,27]

2.3.3. Sen+Mann–Kendall trend analysis

This study employed the Sen+Mann–Kendall trend analysis to assess the spatiotemporal trends in FVC in the Yarkand River Basin from 2000 to 2023. The Mann-Kendall test determined the presence of a significant trend by comparing the order relationships between data points, without relying on the specific distribution of the data, making it suitable for vegetation studies in arid regions. The Theil-Sen slope quantified the magnitude of change, and spatial heterogeneity was analyzed by combining land use types (forest land, grassland, bare land, farmland, etc.) and county/city classifications. The Mann-Kendall test was used to assess significance. Trends were categorized into five levels: highly significant increase ($S > 0$, $p<0.01$), significant increase ($S > 0$, $0.01 \leq p<0.05$), no significant change ($p \geq 0.05$), significant decrease ($S < 0$, $0.01 \leq p<0.05$), and highly significant decrease ($S < 0$, $p<0.01$).[28,29]

2.3.4. Pearson correlation analysis

This study employed Pearson correlation coefficient analysis using the Matrix Laboratory (MATLAB, MathWorks, Inc., United States of America) platform to

investigate the pixel-by-pixel correlation between FVC and climatic factors (temperature and precipitation) in the Yarkand River Basin from 2000 to 2023. The formula of the correlation coefficient was shown in Equation III.

$$r = \frac{\sum_{i=1}^{n}(x_i - \bar{x})(y_i - \bar{y})}{\sqrt{\sum_{i=1}^{n}(x_i - \bar{x})^2 \sum_{i=1}^{n}(y_i - \bar{y})^2}} \quad \text{(III)}$$

where r is the correlation coefficient of x (FVC) and y (temperature or precipitation), and $\bar{x}$ and $\bar{y}$ are the mean values of variables x and y. Based on the calculated results combined with the significant p-value, the correlation was categorized into five classes: highly significant positive correlation ($r \geq 0.5$, $p<0.01$), significant positive correlation ($0.25 \leq r < 0.5$, $p<0.05$), non-significant correlation ($|r| < 0.25$, $p \geq 0.05$), and significant negative correlation ($-0.5 < r \leq -0.25$, $p<0.05$), and highly significant negative correlation ($r \leq -0.5$, $p<0.01$).[30,31]

2.3.5. Persistence analysis

The Hurst exponent, which can be used to predict future trends based on vegetation health index (VHI) time series, is typically calculated using the rescaled range (R/S) analysis method. It characterizes the long-term memory of the VHI time series, ranging from 0 to 1. The Hurst exponent is estimated through several computational relationships (Equations IV to VIII).

$$\frac{R_\tau}{S_\tau} = (c\tau)^H \quad \text{(IV)}$$

$$R_\tau = max_{1 \leq t \leq \tau} X_{t,\tau} - min_{1 \leq t \leq \tau} X_{t,\tau} \quad \text{(V)}$$

$$S_\tau = \left[\frac{1}{\tau}\sum_{t=1}^{\tau}\left(FVC_t - \overline{FVC}_\tau\right)^2\right]^{\frac{1}{2}} (\tau = 1,2,\cdots,n) \quad \text{(VI)}$$

$$X_{t,\tau} = \sum_{t=1}^{t}\left(FVC_t - \overline{FVC}_\tau\right)(1 \leq t \leq \tau) \quad \text{(VII)}$$

$$\overline{FVC}_\tau = \frac{1}{\tau}\sum_{t=1}^{\tau} FVC_t (\tau = 1,2,\cdots,n) \quad \text{(VIII)}$$

where H represents the Hurst exponent, t is the time variable, τ is the time lag, and c is a constant. Values of H within the ranges of $0 < H < 0.5$, $H = 0.5$, and $0.5 < H < 1$ indicate that the VHI time series exhibits anti-persistence (i.e., future trends are opposite to past behavior), random walk behavior (i.e., future changes are uncorrelated with the past), and persistence (i.e., future trends align with past behavior), respectively. Furthermore, as the value of H approaches 1, the persistence strength of the VHI series increases; conversely, as it approaches 0, the anti-persistence intensity strengthens.

3. Results

3.1. Characteristics of the spatial distribution of FVC

The Yarkand River Basin flows from north to south and passes through six counties and cities: Bachu County, Tumushuke City, Makit County, Shache County, Zepu County, and Yecheng County. The FVC in the basin shows noticeable spatial differences, as shown in Figure 2. Overall, it presents a long and narrow vegetation belt running from northeast to southwest, as well as a vegetation belt spanning from northwest to southeast, respectively. The high and medium-high FVC is mainly distributed in the central part of Bachu County, the middle area between the north and south of Tumushuke City, the long and narrow western area of Makit County, the eastern part of Shache County, the vast northern and central regions of Zepu County, the northwestern area connecting Yecheng County and Zepu County, and the mountainous region in the central part.

FVC and its interannual fluctuation were analyzed across county-level administrative units of the Yarkand River Basin (Tables 1 and 2). The results show that the proportion of low coverage in Bachu and Makit is the highest (close to 80%), and the high fluctuation changes are significant (55.9% in Bachu and 72.63% in Makit), indicating that the FVCs in these two counties are poor and have low stability. The proportions of medium-high and high coverage in Zepu and Tumushuke were the highest (61.01% in total for Zepu and 40.51% in total for Tumushuke), among which the high fluctuation change in Zepu was the lowest (25.41%), indicating that its FVC was good and relatively stable. Within the entire area, the proportion of low coverage reached 65.75%, and the proportion of high fluctuation variation was 55.95%, indicating that the overall FVC level in the study area was relatively low and exhibited significant interannual variation.

From 2000 to 2023, the FVC coverage and volatility in the Yarkand River Basin varied significantly among different land use types (Tables 3 and 4). The high coverage of agricultural land accounted for 51.75%, and the medium-high coverage of forest amounted to 60.81%, indicating that irrigation and natural conditions promote the growth of vegetation. Low coverage in bare land accounted for 95.58% and high fluctuation accounted for 74.51%, indicating high environmental

Table 1. Multi-year average fractional vegetation cover share percentage and acreage in different counties and cities

Degree of coverage	Administrative units in the Yarkand River Basin (%; km²)						
	Bachu County	Makit County	Shache County	Tumushuke City	Yecheng County	Zepu County	Entire area
Low coverage	79.80%; 14,683.20	79.95%; 8,714.55	54.82%; 4,910.23	20.04%; 386.17	59.34%; 16,971.24	20.25%; 200.07	65.75%; 45,875.09
Low to medium coverage	8.83%; 1,624.72	5.43%; 591.87	14.91%; 1,335.49	25.61%; 493.50	26.43%; 7,558.98	10.51%; 103.84	16.78%; 11,707.74
Medium coverage	3.20%; 588.80	2.93%; 319.37	7.17%; 642.22	13.85%; 266.89	7.09%; 2,027.74	8.24%; 81.41	5.62%; 3,921.19
Medium to high coverage	3.33%; 612.72	4.86%; 529.74	10.91%; 977.21	20.02%; 385.79	4.24%; 1,212.64	27.21%; 268.83	5.71%; 3,983.98
High coverage	4.83%; 888.72	6.83%; 744.47	12.19%; 1,091.86	20.49%; 394.84	2.89%; 826.54	33.80%; 333.94	6.14%; 4,284.00

Table 2. Share percentage and acreage of fractional vegetation cover coefficient of fluctuation in different counties and cities

Degree of fluctuation	Administrative units in the Yarkand River Basin (%; km²)						
	Bachu County	Makit County	Shache County	Tumushuke City	Yecheng County	Zepu County	Entire area
Low fluctuation change	3.38%; 621.92	3.49%; 380.41	5.39%; 482.78	6.50%; 125.26	3.33%; 952.38	15.66%; 154.72	3.90%; 2,721.11
Lower fluctuation change	9.16%; 1,685.44	5.95%; 648.55	14.85%; 1,330.12	17.98%; 346.47	12.64%; 3,615.04	37.09%; 366.45	11.46%; 7,995.87
Medium fluctuation change	12.32%; 2,266.88	5.91%; 644.19	13.53%; 1,211.88	20.64%; 397.73	13.86%; 3,963.96	14.57%; 143.95	12.36%; 8,623.82
Higher fluctuation change	19.23%; 3,538.32	12.02%; 1,310.18	19.36%; 1,734.08	23.11%; 445.33	15.03%; 4,298.58	7.27%; 71.83	16.33%; 11,393.77
High fluctuation change	55.90%; 10,285.60	72.63%; 7,916.67	46.88%; 4,199.04	31.76%; 612.02	55.12%; 15,764.32	25.41%; 251.05	55.95%; 39,037.43

Table 3. Multi-year average fractional vegetation cover share percentage and acreage in different land use types

Degree of coverage	Administrative units in the Yarkand River Basin (%; km²)					
	Farmland	Forests	Grassland	Bare land	Others	Entire area
Low coverage	0.85%; 64.07	2.06%; 0.83	26.56%; 4,146.97	95.58%; 40,918.22	14.35%; 469.02	65.75%; 45,874.50
Low to medium coverage	5.32%; 403.03	6.48%; 2.62	42.50%; 6,635.99	4.12%; 1,764.40	85.13%; 2,781.72	16.78%; 11,706.89
Medium coverage	9.72%; 736.80	23.45%; 9.49	19.37%; 3,024.00	0.23%; 96.46	0.31%; 10.03	5.62%; 3,923.86
Medium to high coverage	32.37%; 2,454.50	60.81%; 24.60	9.22%; 1,439.56	0.06%; 26.01	0.13%; 4.20	5.71%; 3,984.98
High coverage	51.75%; 3,923.54	7.19%; 2.91	2.36%; 367.74	0.01%; 4.15	0.08%; 2.63	6.14%; 4,281.77

sensitivity. Grassland has 42.50% of low cover and 34.90% of high fluctuation, which may be affected by precipitation changes. The proportion of low coverage in the whole area is 65.75%, and the proportion of high

Table 4. Share percentage and acreage of fractional vegetation cover coefficient of fluctuation in different land use types

Degree of fluctuation	Administrative units in the Yarkand River Basin (%; km²)					
	Farmland	Forests	Grassland	Bare land	Others	Entire area
Low fluctuation change	23.02; 1,741.53	22.18; 11.82	2.71; 423.27	0.73; 312.08	7.49; 243.17	3.90; 2,719.20
Lower fluctuation change	33.55; 2,538.08	46.16; 24.60	13.70; 2,138.89	4.50; 1,919.62	39.25; 1,274.88	11.46; 7,994.74
Medium fluctuation change	16.81; 1,271.58	21.24; 11.32	19.57; 3,055.42	6.90; 2,945.40	39.03; 1,267.78	12.36; 8,624.87
Higher fluctuation change	13.10; 991.01	7.98; 4.25	29.12; 4,547.28	13.36; 5,704.27	0.63; 20.63	16.33; 11,394.23
High fluctuation change	13.52; 1,022.82	2.44; 1.30	34.90; 5,449.99	74.51; 31,799.37	13.60; 441.65	55.95; 39,038.96

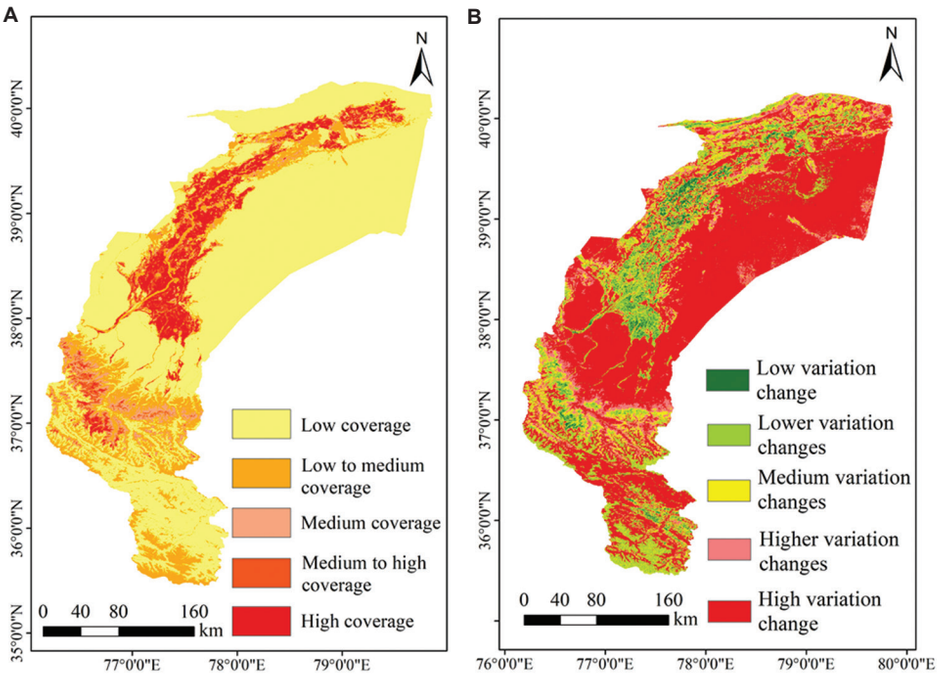

Figure 2. Multi-year data of fractional vegetation cover in the Yarkand River Basin from 2000 to 2023. (A) Mean. (B) Fluctuation.

fluctuation is 55.95%, reflecting the vulnerability of vegetation in arid regions. The lower fluctuation of the forest accounted for 46.16%, with the best stability, which may be related to the adaptation of forest trees. Bare land cover was low and fluctuating, with high difficulty in ecological restoration. The study reveals the role of land use types in regulating the distribution and stability of FVC, providing a basis for environmental management. In the future, it will be necessary to optimize the bare land restoration strategy in combination with land use dynamics to enhance the regional ecological stability.

3.2. Interannual trends of FVC

Between 2000 and 2023, FVC in the Yarkand River Basin exhibited significant spatial and temporal changes (Figure 3). The FVC of the whole area increased from 0.16 to 0.22 and stabilized at 0.21–0.23 after 2010, indicating an overall improvement of FVC. Based on the results of linear regression analysis, the spatial and temporal evolution of FVC in the study area showed significant regional differentiation. Tumushuke showed the strongest growth trend (slope = 0.009, R^2 = 0.819), with its FVC increasing continuously from 0.39 in 2000

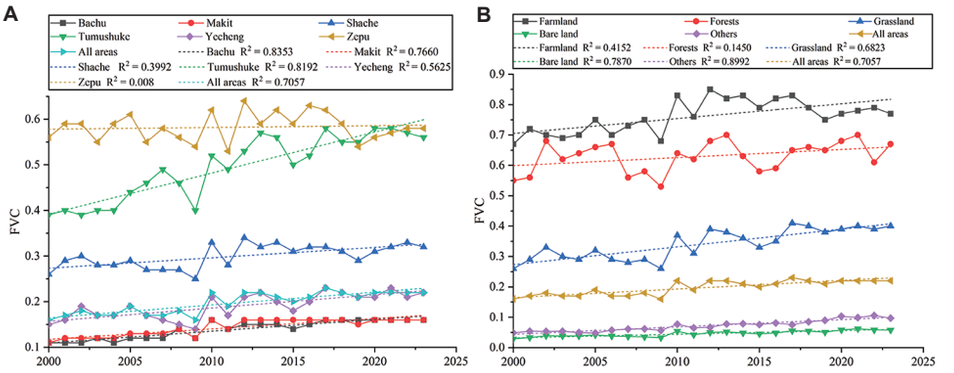

Figure 3. Evolution of FVC in different categories of the Yarkand River Basin. (A) Evolution of FVC in other administrative regions. (B) Evolution of FVC in various land use types.
Abbreviation: FVC: Fractional vegetation cover.

to 0.56 in 2023. Bachu (slope = 0.0026, $R^2 = 0.835$) and Makit (slope = 0.0023, $R^2 = 0.766$) exhibited relatively slow growth but a high goodness-of-fit to the model. It is noteworthy that the Zepu region ($R^2 = 0.008$) lacks statistical significance in its trend due to the high FVC levels (0.56–0.64) over a long period.

On the whole-area scale, FVC showed a stable upward trend (slope = 0.0028, $R^2 = 0.706$), which was consistent with the pattern of change in most counties and cities. However, the model fits of Shache ($R^2 = 0.399$) and Yecheng ($R^2 = 0.563$) were relatively low, suggesting that several factors, such as agricultural expansion or occasional natural disasters, may have interfered with the long-term change pattern of FVC in these regions.

Under different land use type classifications, farmland FVC increased from 0.67 to 0.77, peaking at 0.83 in 2010, reflecting the irrigation management effect; forest FVC increased steadily from 0.55 to 0.70, showing natural adaptation; grassland FVC increased from 0.26 to 0.40, stabilizing after 2017, benefiting from improved water resources; and bare land FVC increased from 0.03 to 0.06, with slow growth and limited ecological restoration; other types FVC increased from 0.05 to 0.10, with a rapid increase after 2020, probably related to land use adjustment. The period from 2000 to 2010 was one of rapid growth, and from 2010 to 2023, the growth leveled off, suggesting that management measures were effective in the early years. The differences in land use types reflect the combined drive of artificial interventions and natural conditions, and the slow growth of bare land requires attention to ecological vulnerability.

From 2000 to 2023, the FVC trend (Sen+Mann–Kendall analysis) in the Yarkand River Basin showed significant regional differentiation (Figure 4). The degree of FVC change in the counties and cities of the Yarkand River Basin is shown in Table 5, with a highly significant increase ($p<0.01$) accounting for 72.55% of the total area, a significant increase of 15.94%, and a decrease of only 8.32%, indicating an overall improvement in FVC. Makit County had the highest percentage of highly significant increase (77.93%) and decrease of only 5.67%, indicating the most significant improvement in FVC. Yecheng County had a highly significant increase of 73.83% and a decrease of 4.67%, indicating significant vegetation recovery. Tumushuke City and Bachu County had an increase of 82.13% and 89.86%, respectively (decrease of 9.60% and 8.24%), with improvement dominating. Shache County experienced a highly significant increase of 71.51% but a decrease of 19.41%, reflecting the coexistence of degradation and improvement, which may be influenced by human interference. Zephyr County experienced a highly significant increase of 47.35% and a highly significant decrease of 40.94%, indicating a balanced trend with both positive and negative outcomes.

The trend of FVC change in the Yarkand River Basin showed significant differences among different land use types, as shown in Table 6. Grassland and bare land accounted for 80.22% and 78.40% of the highly significant increase, indicating that the natural vegetation recovery was evident. Forest accounted for 58.80% of the highly significant increase, and the increase was superior, which may be due to the benefit of ecological protection. Farmland accounted for 51.86% of the highly significant increase; however, the highly significant decrease of 34.28% indicated that management effectiveness and degradation coexist. Other types of significant increase accounted for 85.93%, the decrease v was extremely low, and

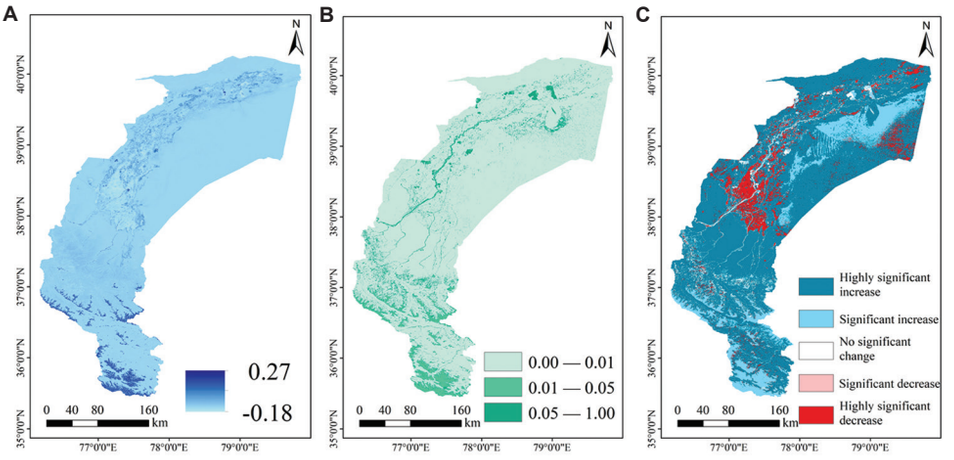

Figure 4. Spatial distribution of annual trends of fractional vegetation cover in the Yarkand River Basin from 2000 to 2023. (A) Slope of change. (B) *p*-value. (C) Zone of significant change.

Table 5. The extent of change in share percentage and acreage of fractional vegetation cover in different counties and cities

Degree of coverage	Administrative units in the Yarkand River Basin (%; km²)						
	Bachu County	Makit County	Shache County	Tumushuke City	Yecheng County	Zepu County	Entire area
Highly significant increase	69.44; 12,763.69	77.93; 8,507.49	71.51; 6,374.62	70.79; 1,353.02	73.83; 21,114.62	47.35; 476.47	72.55; 50,620.16
Significant increase	20.42; 3,753.18	14.57; 1,590.98	4.70; 418.89	11.34; 216.70	17.77; 5,081.43	5.11; 51.40	15.94; 11,120.30
No significant change	1.91; 351.46	1.82; 199.14	4.38; 390.67	8.28; 158.24	3.73; 1,066.94	6.17; 62.06	3.20; 2,229.99
Significant decrease negative increase	0.07; 12.73	0.09; 10.31	0.20; 17.55	0.49; 9.38	0.07; 20.09	0.44; 4.39	0.11; 74.47
Highly significant decrease	8.17; 1,501.06	5.58; 609.59	19.21; 1,712.87	9.11; 174.07	4.60; 1,314.15	40.94; 411.94	8.21; 5,727.08

Table 6. The extent of change in share percentage and acreage of fractional vegetation cover in different land use types

Degree of coverage	Administrative units in the Yarkand River Basin (%; km²)					
	Farmland	Forests	Grassland	Bare land	Others	Entire area
Highly significant increase	51.86; 3,968.19	58.80; 31.34	80.22; 12,321.99	78.40; 33,508.53	7.23; 236.95	72.55; 50,620.16
Significant increase	9.67; 739.63	8.89; 4.74	5.94; 912.07	15.40; 6,582.78	85.93; 2,816.53	15.94; 11,120.30
No significant change	3.78; 289.19	11.20; 5.97	7.63; 1,172.34	1.35; 577.66	5.89; 192.96	3.20; 2,229.99
Significant decrease	0.42; 31.86	0.69; 0.37	0.24; 36.57	0.02; 7.09	0.01; 0.35	0.11; 74.47
Highly significant decrease	34.28; 2,623.45	20.42; 10.88	5.97; 917.11	4.83; 2,065.22	0.95; 31.04	8.21; 5,727.08

the growth was stable. The growth trend of the entire area was consistent with the development of the oasis and water resource management initiatives after 2000. However, the high proportion of decline of farmland

suggested the risk of localized degradation. Differences in land use types reflected the combined drive of artificial intervention and natural conditions, with bare land and grassland showing significant growth, and farmland requiring optimized management.

3.3. Sustainability analysis of FVC

The Hurst index was employed to analyze the long-term memory and persistence of the FVC time series, with results shown in Figure 5. At the regional scale, the annual mean FVC exhibited strong positive persistence, with a Hurst coefficient of 0.81. To validate this finding, the climacogram method was additionally applied, yielding a similar value of 0.896. The close agreement between the R/S and climacogram methods confirmed the robustness of the persistence detected at the regional level. In contrast, the mean Hurst coefficient across the entire raster grid was 0.44, indicating anti-persistence at the local scale, where FVC changes were more likely to reverse existing trends. This spatial divergence reflects the region's complex heterogeneity: oases, supported by irrigated agriculture, typically show higher FVC and local persistence ($H > 0.5$); deserts, constrained by scarce precipitation and significant interannual variability, exhibit very low FVC and anti-persistence ($H < 0.5$); and mountainous areas, shaped by complex topography and limited water availability, display unstable FVC dynamics with generally lower Hurst values. Areas with persistently low FVC or data gaps may further reduce the mean coefficient, contributing to the overall anti-persistent trend at the local scale.

In contrast, the Hurst coefficient of 0.81 (>0.5) for the annual mean FVC indicated strong positive persistence, with FVC changes tending to maintain existing trends (e.g., continuous increase). By spatially averaging FVC across the study area, the differences among oases, deserts, and mountains were smoothed out, highlighting the overall regional trend. In recent years, the Yarkand River Basin has benefited from the expansion of oasis agriculture, afforestation policies, and ecological restoration measures (e.g., windbreak and sand-fixation forest construction), leading to a likely sustained increase in regional mean FVC, particularly in oasis areas supported by irrigation, which enhances FVC stability. The influence of deserts and mountains was diminished after spatial averaging, resulting in a smoother time series for the annual mean FVC, reflecting long-term ecological stability at the regional scale.

From a spatial distribution perspective, the FVC in the plain areas of the Yarkand River Basin generally exhibited positive and strong positive persistence. In contrast, in mountainous regions, it predominantly showed anti-persistence and strong anti-persistence. This is primarily because plain areas, as key regions for irrigated agriculture, benefit from effective water resource management and optimized irrigation

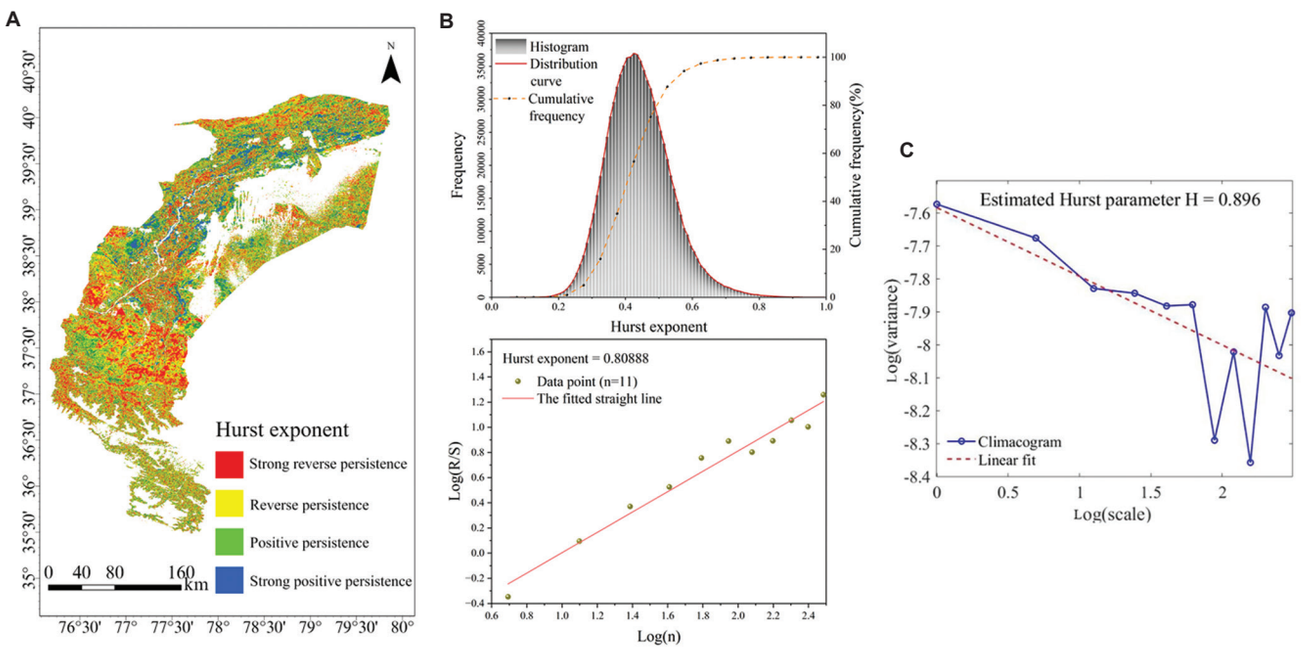

Figure 5. Annual fractional vegetation cover change trends in the Yarkand River Basin from 2000 to 2023. (A) Distribution. (B) Characteristics of sustainability. (C) Climacogram.

techniques, providing favorable conditions for vegetation growth. In addition, farmland protection policies and land reclamation measures create a conducive environment for the development of vegetation. However, in mountainous areas, complex terrain combined with harsh climatic conditions and surface exposure due to snowmelt restricts vegetation growth potential.

The Hurst coefficients in the Yarkand River Basin reflect the impact of spatial heterogeneity on vegetation dynamics. The positive persistence in oasis areas was offset by the anti-persistence in desert and mountainous areas, resulting in a lower mean Hurst coefficient across the entire grid. Desert areas, affected by extreme aridity and wind erosion, experienced significant fluctuations in FVC with easily reversible trends, while mountainous areas, constrained by terrain and climate, exhibited unstable changes in FVC. These local-scale anti-persistent trends, combined with the positive persistence in oasis areas, shaped the spatial distribution of the Hurst coefficient across the region. The regional-scale positive persistence (H = 0.81) highlighted the stabilizing contribution of oasis agriculture and ecological protection measures to overall FVC.

The mean Hurst coefficient for the entire grid (H = 0.44) underscored the spatial heterogeneity and ecological vulnerability of FVC at the local scale in the Yarkand River Basin. The positive persistence in oasis areas indicated that irrigated agriculture and ecological restoration measures (e.g., afforestation) support long-term FVC stability, while the anti-persistence in desert areas reflected constraints from aridity and wind erosion, and mountainous areas were limited by terrain and precipitation, making FVC susceptible to short-term disturbances (e.g., drought, floods). The Hurst coefficient of 0.81 for the annual mean FVC suggested long-term stability of FVC at the regional scale, likely driven by the dominant role of oasis areas and regional ecological policies, such as afforestation, oasis expansion, and optimized water resource management. Climatic factors (e.g., precipitation fluctuation, temperature rise) and human activities (e.g., agricultural reclamation, overgrazing) further exacerbate spatial heterogeneity, shaping the distinct FVC dynamics across different geomorphic units.

3.4. Analysis of drivers of FVC

3.4.1. Spatial distribution and interannual fluctuation of climate factors

The multi-year average temperature data in counties and cities in the Yarkand River Basin showed obvious spatial differentiation patterns (Figure 6). The spatial

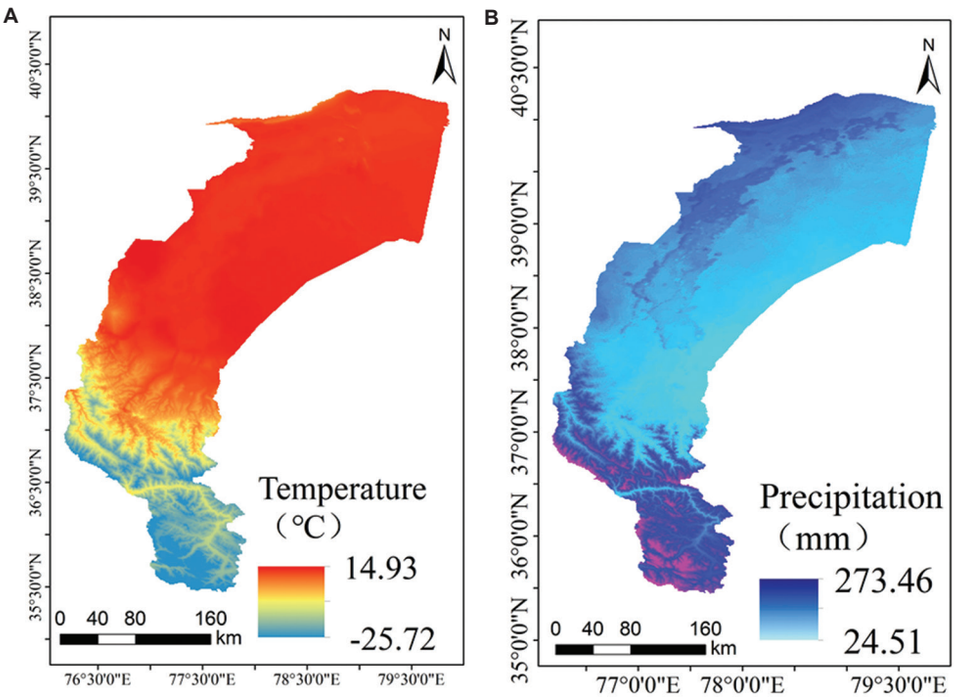

Figure 6. Spatial distribution of the average status of climate factors in the Yarkand River Basin from 2000 to 2023. (A) Spatial distribution of multi-annual mean temperature. (B) Spatial distribution of multi-year precipitation.

interannual variations of climate factors in counties and cities are shown in Figure 7, with higher and least varied temperatures in Bachu County (7.4–14°C), Tumushuke City (11.6–13.3°C), Makit County (13–14.2°C), and Zepu County (13.3–14.4°C). The regional differences in the multi-year mean temperatures in Shache County (−4.8–14.9°C) and Yecheng County (−25.7–14.5°C) were evident, which may be related to the fact that some regions of higher terrain in the northern part of the county were prone to accumulating cold air during winter.[32] Overall, the temperature distribution in the region showed three characteristics: first, the temperature in the plain oasis area generally maintained between 11 and 14°C; second, the temperature fluctuated greatly in the northern region close to the Tianshan Mountains; and third, the temperature varied exceptionally with altitude in the southern Kunlun Mountains. This distribution pattern reflected both the general geographic context and the profound influence of local topography on temperature.[33] Follow-up studies can be conducted to further clarify the specific role of topographic factors in temperature distribution by combining the elevation locations of specific weather stations.

The multi-year average precipitation of the counties and cities in the Yarkand River Basin showed noticeable spatial differences and local peculiarities. Overall, the region was extremely arid, with annual precipitation generally lower than 90 mm, below the national average, except for high values in Yecheng County. In terms of distribution trends, Bachu County and Tumushuke City in the north (34.1–85.3 mm and 40.4–65.7 mm) were slightly higher than Makit County in the south (31.8–61 mm), but Yecheng County (24.5–273.5 mm), due to the proximity of the Kunlun Mountains terrain uplift effect, showed a high value of precipitation rarely seen in the southern Xinjiang, which was probably affected by strong convection in the mountainous areas or the residual water vapor of the Indian Ocean monsoon.[34] The significant difference in precipitation between Shache County (33.9–89.7 mm) and the neighboring Zephyr County (35.9–47.9 mm) may be related to microtopography and oasis effects.[35] Overall, precipitation in the region mainly relied on weak water vapor from the westerly wind belt, while basin topography exacerbated drought. Notably, only Yecheng County formed a unique precipitation pattern due to changes in the elevation gradient.

The trend of temperature and precipitation changes under different land use types in the Yarkand River Basin is shown in Figure 8. Farmland and bare land exhibited the largest increase (1.07°C and 1.03°C, respectively), while other types had the smallest decrease (0.74°C), reflecting regional temperature rise differences. Precipitation increased from 35.01 mm to 49.03 mm, with peaks of 68.52 mm and 80.00 mm in 2003 and 2005, and a significant increase in other types (19.03 mm), indicating improved water resources.[36] Farmland and forest temperature increases were correlated with steady FVC increases. Similarly, an increase in grassland precipitation was consistent with the rise in FVC, while the increase in bare land temperature may suppress FVC. High precipitation but fluctuating FVC in other land types suggested low utilization efficiency (Figures 3, 7, and 8). The trends indicated that warming temperatures and increased precipitation together drove improvements in vegetation, with land use types modulating the intensity of the response.

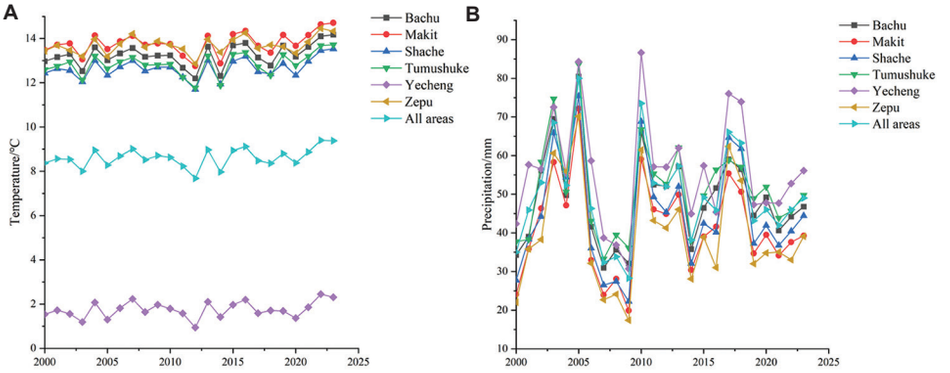

Figure 7. Interannual variation of climatic factors in counties and cities of the Yarkand River Basin. (A) Interannual variation in temperature factors by county and city. (B) Interannual variation in precipitation factors by county and city area.

3.4.2. Correlation analysis between FVC and climate factors

Based on *p*-value significance tests, the correlation between FVC and climate factors in the Yarkand River Basin from 2000 to 2023 is shown in Figures 9 and 10. The correlations for each county are shown in Tables 7 and 8. The positive correlation (extremely significant and significant) between FVC and temperature was the highest in Yecheng County (27.89%), possibly due to the extended vegetation growth cycle caused by rising temperatures, especially in spring, which improves coverage.[37] Zepu County had a negative correlation of 39.44%, while Shache County correlated of 30.30%. High temperatures can exacerbate water evaporation and hinder vegetation growth, particularly during drought years.[38] The proportion of non-significant correlations in Tumushuke City was 50.24%, while Bachu County and Makit County showed balanced positive and negative correlations (27.71% vs. 25.84% and 25.20% vs. 23.79%, respectively), indicating that the impact of temperature on FVC varies by location.[39] Across the entire region, 26.64% showed a positive correlation and 24.52% showed a negative correlation, reflecting the complex effects of temperature.[40]

FVC showed a significant positive correlation with precipitation in Shache County and Yecheng County (62.12% and 60.33%, respectively), with a regional average of 51.77%, indicating that increased precipitation significantly promotes FVC, particularly in water-sensitive areas, possibly due to precipitation that optimized soil moisture.[37] In Tumushuke City, the proportion of negative correlations was 19.52%, and the proportion of non-significant correlations was 64.75%, possibly due to excessive precipitation causing soil erosion or vegetation adapting to drought, with precipitation changes disrupting ecological balance.

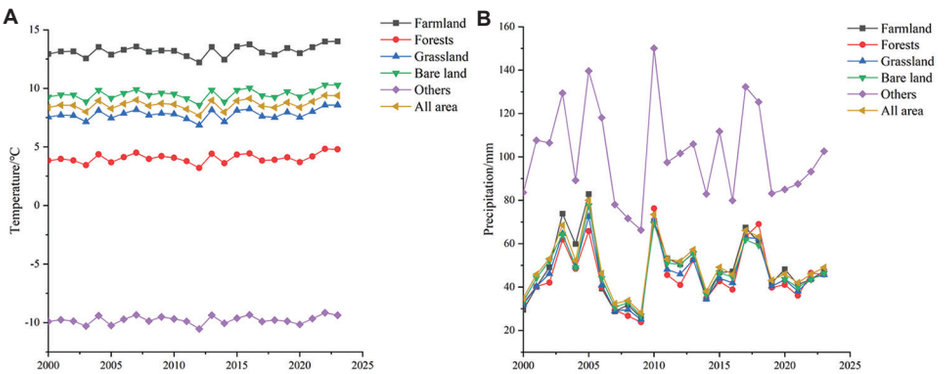

Figure 8. Interannual variation of climatic factors by land use types in the Yarkand River Basin. (A) Interannual fluctuation of temperature factors under different land use types. (B) Interannual fluctuation in precipitation factors for different land use types.

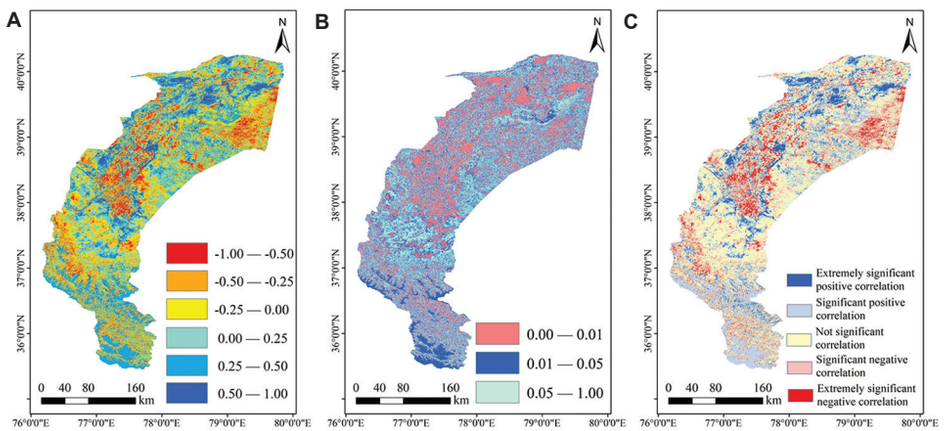

Figure 9. Correlation analysis between fractional vegetation cover changes and annual average temperature in the Yarkand River Basin from 2000 to 2023. (A) Correlation between fractional vegetation cover and annual average temperature. (B) *p*-value. (C) Significant change area.

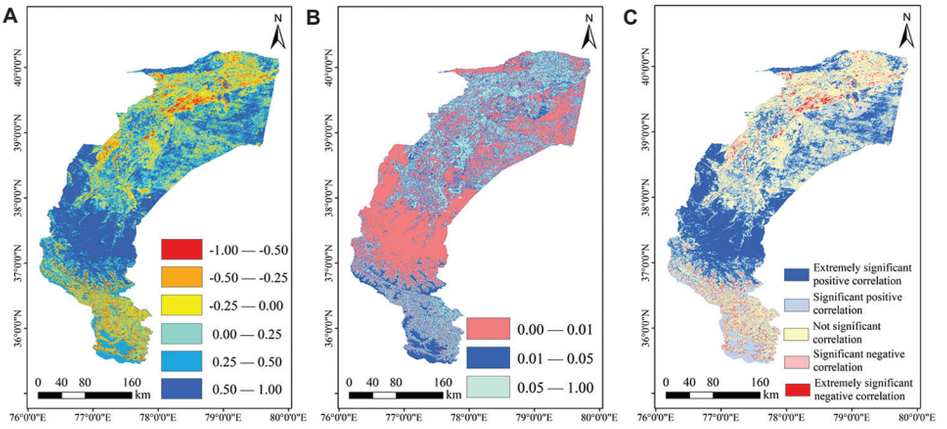

Figure 10. Correlation analysis between fractional vegetation cover changes and annual precipitation averages in the Yarkand River Basin from 2000 to 2023. (A) Correlation between fractional vegetation cover and annual precipitation. (B) *p*-value. (C) Significant change area.

Table 7. Acreage and share percentage of various correlations between fractional vegetation cover and temperature in different counties and cities

Relevance	Administrative units in the Yarkand River Basin (%; km²)						
	Bachu County	Makit County	Shache County	Tumushuke City	Yecheng County	Zepu County	Entire area
Extremely significant positive correlation	15.32; 2,815.38	13.21; 1,442.12	12.50; 1,114.18	16.52; 315.71	8.93; 2,553.06	15.84; 159.50	12.05; 8,405.63
Significant positive correlation	12.39; 2,277.55	11.99; 1,308.92	9.52; 848.50	11.98; 228.86	18.96; 5,422.75	9.00; 90.63	14.59; 10,177.10
Non-significant correlation	45.85; 8,427.78	51.02; 5,570.20	47.69; 4,250.97	50.24; 960.09	50.65; 14,483.76	35.72; 359.59	48.85; 34,080.60
Significant negative correlation	17.52; 3,220.52	14.33; 1,565.03	18.56; 1,654.38	11.49; 219.61	15.23; 4,354.06	23.16; 233.11	16.13; 11,253.34
Extremely significant negative correlation	8.92; 1,638.96	9.46; 1,032.40	11.74; 1,046.56	9.77; 186.70	6.24; 1,783.43	16.28; 163.91	8.39; 5,855.34

Table 8. Acreage and share percentage of various correlations between fractional vegetation cover and precipitation in different counties and cities

Relevance	Administrative units in the Yarkand River Basin (%; km²)						
	Bachu County	Makit County	Shache County	Tumushuke City	Yecheng County	Zepu County	Entire area
Extremely significant positive correlation	26.91; 4,948.81	24.38; 2,661.64	49.69; 4,429.74	7.90; 150.99	41.01; 11,728.25	23.27; 234.23	34.77; 24,261.34
Significant positive correlation	17.57; 3,230.48	17.11; 1,867.84	12.43; 1,108.05	7.84; 149.81	19.32; 5,523.78	18.11; 182.32	17.00; 11,861.97
Non-significant correlation	42.98; 7,902.44	51.66; 5,640.25	30.26; 2,698.09	64.75; 1,237.78	28.69; 8,205.97	52.65; 530.04	37.91; 26,449.53
Significant negative correlation	10.12; 1,861.33	5.54; 605.15	6.37; 567.68	15.77; 301.39	8.07; 2,307.02	4.93; 49.60	8.02; 5,598.30
Extremely significant negative correlation	2.41; 443.88	1.32; 144.10	1.25; 111.50	3.75; 71.68	2.91; 832.34	1.04; 10.49	2.29; 1,600.86

Zepu County had a non-significant correlation of 52.65%, with weak precipitation effects, possibly due to vegetation already adapting to the current precipitation pattern.[39] In Bachu County and Makit County, the proportion of positive correlations was 44.48% and 41.49%, respectively, while the proportion of negative correlations was low (12.53% and 6.86%, respectively), indicating that precipitation moderately promotes vegetation.[37]

Correlation analysis between FVC and climate factors in the Yarkand River Basin from 2000 to 2023 showed high proportions of positive correlations between FVC and precipitation in Shache County and Yecheng County (62.12% and 60.33%, respectively), with Yecheng County exhibiting the strongest positive correlation with temperature (27.89%). In Zepu County and Tumushuke City, negative correlations and insignificant correlations dominated, reflecting regional differentiation. From 2000 to 2023, the correlations between FVC and temperature and precipitation under different land-use types in the Yarkand River Basin are presented in Tables 9 and 10. The correlation between FVC and temperature shows that farmland and forest have a high proportion of extremely significant negative correlations (21.97% and 20.45%, respectively), possibly due to high temperatures inhibiting vegetation growth.[39] Grasslands and bare land showed non-significant correlations exceeding 50% (50.91% and 49.58%, respectively), indicating a strong level of adaptability. Other land use types exhibited significant positive correlations at 71.26%, reflecting the warming-enhancing effect. Across the entire study area, there was a highly significant negative correlation of 8.39% and a significant positive correlation of 14.59%. In the correlation between FVC and precipitation, grasslands and forests showed a high proportion of highly

Table 9. Acreage and share percentage of various correlations between fractional vegetation cover and temperature in different land use types

Relevance	Administrative units in the Yarkand River Basin (%; km²)					
	Farmland	Forests	Grassland	Bare land	Others	Entire area
Extremely significant positive correlation	5.99; 458.36	3.84; 1.58	11.94; 1,864.92	13.61; 5,828.13	7.33; 244.19	12.05; 8,405.63
Significant positive correlation	9.03; 691.32	7.01; 2.89	11.23; 1,753.75	13.48; 5,771.08	71.26; 2,374.42	14.59; 10,177.10
Non-significant correlation	41.61; 3,184.27	40.89; 16.84	50.91; 7,950.35	49.58; 21,228.53	14.24; 474.57	48.85; 34,080.60
Significant negative correlation	21.40; 1,637.63	27.81; 11.45	18.22; 2,844.68	16.58; 7,096.71	3.69; 123.07	16.13; 11,253.34
Extremely significant negative correlation	21.97; 1,681.33	20.45; 8.42	7.70; 1,202.06	6.75; 2,888.92	3.48; 115.96	8.39; 5,855.34

Table 10. Acreage and share percentage of various correlations between fractional vegetation cover and precipitation in different land use types

Relevance	Administrative units in the Yarkand River Basin (%; km²)					
	Farmland	Forests	Grassland	Bare land	Others	Entire area
Extremely significant positive correlation	23.54; 1,783.11	46.75; 19.07	47.91; 7,328.56	34.73; 14,808.27	5.19; 169.69	34.77; 24,261.34
Significant positive correlation	18.87; 1,429.16	21.29; 8.68	9.66; 1,477.72	15.24; 6,498.38	71.78; 2,346.08	17.00; 11,861.97
Non-significant correlation	51.19; 3,876.49	30.29; 12.35	30.75; 4,704.05	39.41; 16,805.70	12.59; 411.48	37.91; 26,449.53
Significant negative correlation	5.61; 424.73	1.57; 0.64	9.08; 1,389.17	8.29; 3,534.86	6.39; 209.00	8.02; 5,598.30
Extremely significant negative correlation	0.79; 59.72	0.10; 0.04	2.59; 396.77	2.33; 991.66	4.05; 132.37	2.29; 1,600.86

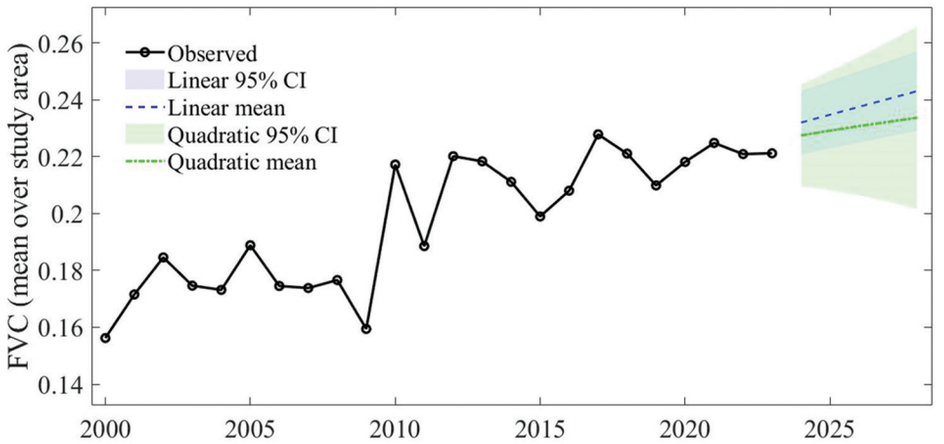

Figure 11. Annual FVC (2000–2023) and 5-year forecasts (2024–2028)
Abbreviations: CI: Confidence interval; FVC: Fractional vegetation cover.

significant positive correlations (47.91% and 46.75%), indicating that precipitation drives vegetation recovery. For farmland, there was a highly significant positive correlation of 23.54% and a significant negative correlation of 5.61%, reflecting a complex response. In terms of bare land, there was a positive correlation of 34.73% and a negative correlation of 10.62%, indicating significant fluctuations. Other land types showed a significant positive correlation of 71.78%, suggesting significant gains. The overall region showed a highly significant positive correlation of 12.05% and a negative correlation of 2.89%. The study reveals the differential effects of climate factors on FVC, with grasslands and forests benefiting from precipitation, farmland requiring optimized management, and bare land exhibiting low stability.

3.5. Short-term regression-based forecast of FVC dynamics

Based on the annual FVC series from 2000 to 2023, both linear and quadratic regression models were applied to forecast the short-term dynamics of FVC for 2024–2028, as shown in Figure 11. The linear regression model indicated a gradual increase in FVC from approximately 0.232 in 2024 to 0.243 in 2028. The quadratic model produced slightly lower estimates, from about 0.227 in 2024 to 0.234 in 2028, suggesting a modest deceleration in the rate of increase. In both cases, the 95% confidence intervals remained narrow, indicating relatively robust short-term forecasts. Overall, the results suggest that FVC in the study area will remain relatively stable with a slight upward trend over the next 5 years.

In particular, the forecasts for the first 2 years highlight the stability of the short-term dynamics. In 2024, the linear regression model predicts an FVC of approximately 0.232 (95% confidence interval [CI]: 0.221–0.243), while the quadratic model yielded a similar value of 0.227 (95% CI: 0.210–0.245). In 2025, both models projected a slight increase, with values of 0.235 (linear) and 0.229 (quadratic), again within narrow confidence intervals. These results suggest that the study area will experience only modest changes in vegetation cover at the beginning of the forecast period, reinforcing the conclusion of overall stability and a gradual upward trend.

4. Discussion

This study analyzed changes in FVC in the Yarkand River Basin based on the MODIS NDVI data from 2000 to 2023, revealing significant spatiotemporal heterogeneity. Before 2000, the average FVC value was 0.16–0.17, with significant fluctuations, reflecting the impacts of arid climate and early human activities. After 2000, due to oasis development and water resource management, FVC increased significantly, stabilizing at 0.21–0.23 after 2010, with approximately 70% of the area showing significant growth ($p < 0.05$, Sen+Mann–Kendall test). The FVC in Tumushuke City increased from 0.39 to 0.58, and the proportion of growth in Makit County reached 75%, indicating significant ecological restoration achievements. However, a local decline of approximately 8% occurred in 2022–2023, potentially related to the abnormal high temperature of 14.01°C, highlighting the regional vulnerability. The Hurst index analysis of the study area's time series reveals its long-term memory and trend persistence. This additional analysis using the climacogram method[41] addressed

the methodological concerns, confirming that the persistence estimated by the R/S approach is reliable and that both methods provide consistent evidence of strong long-term memory in regional FVC dynamics. Results show that the Hurst coefficient for the annual mean FVC is 0.81 (>0.5), indicating strong positive persistence at the regional scale, where FVC changes tend to maintain existing trends (e.g., continuous increase). In contrast, the mean Hurst coefficient for the entire raster grid is 0.44 (<0.5), suggesting anti-persistence at the local scale. This discrepancy arises from the spatial heterogeneity among oases, deserts, and mountainous areas within the region. Despite the overall positive persistence trend, local-scale complexities reduce the mean Hurst coefficient across the entire grid.

The similarity between the Hurst parameters of FVC (0.81–0.90) and those reported for climatic processes, such as temperature and precipitation (e.g., Dimitriadis *et al*.,[42] H ≈ 0.83), suggests a potential linkage between vegetation dynamics and the long-term memory of climate drivers. This resemblance suggests that vegetation cover does not evolve in isolation but may exhibit similar persistence properties to climatic variability at the macroscale. Such findings highlight the coupled and enduring interactions between vegetation and climate in arid ecosystems. Future research could therefore extend Hurst analysis to temperature and precipitation processes in the Yarkand River Basin, providing a more comprehensive understanding of the co-evolution and feedback mechanisms between climate and vegetation.

In terms of climate drivers, the temperature increased from 8.4°C to 9.4°C (an increase of approximately 1°C), promoting an increase in farmland FVC from 0.67 to 0.77 (high coverage of roughly 50%), possibly due to the extended growing season caused by the temperature increase. The FVC of bare land increased from 0.03 to 0.06, indicating a slight upward trend, particularly in Zepu and Bachu counties (low coverage of approximately 80% and high volatility of about 70%), possibly due to accelerated soil moisture evaporation caused by rising temperatures. Precipitation increased from 35 mm to 49 mm, with a peak of approximately 80 mm in 2005, significantly driving grassland FVC from 0.26 to 0.40 (increase of roughly 80%), particularly in Bachu and Tumushuke counties, consistent with improved soil moisture due to increased precipitation. The decrease of approximately 30% in farmland may be related to salinization caused by over-irrigation, contrasting with the increase of approximately 45% in grasslands, reflecting the differing responses of different land-use types.

County-level heterogeneity further supports these trends. FVC in Yecheng County was positively correlated with temperature by approximately 25%, while in Shache County, it was positively correlated with precipitation by approximately 60%, indicating that southern counties and cities benefit from improved water and heat conditions. In Zepu County, FVC was negatively correlated with temperature by approximately 40%, possibly due to high temperatures exacerbating drought stress. The differing responses of forested areas (with medium to high coverage of roughly 60% and fluctuation of approximately 2%) and bare land validate this mechanism.

The results of this study are highly consistent with recent research by Piao *et al.*,[3] which reported that climate change and human activities drive global vegetation greening. This is consistent with the growth trend of FVC in this study, emphasizing the roles of precipitation and oasis management. Wei *et al.*[43] analyzed the impact of climate fluctuation on vegetation growth, consistent with the increase in FVC in farmland. Cao *et al.*[44] found that drought exacerbates agricultural stress, aligning with the decline trend in farmland. Wang *et al.*[45] used MODIS data to analyze land surface temperature and vegetation dynamics, supporting the high-temperature stress mechanism in Zepu County. Qi *et al.*[46] investigated precipitation patterns and vegetation recovery, supporting the mechanism of FVC increase in grasslands. Urban *et al.*[47] explored the interactive effects of climate and land use, supporting the overall driving mechanism. Gao *et al.*[48] emphasize the short-term response of arid zone vegetation to climate fluctuation, consistent with the local decline observed in 2022–2023.

The findings of this study on FVC dynamics in the Yarkand River Basin have been corroborated by related research conducted in other arid and semi-arid regions, thereby reinforcing the robustness and applicability of our conclusions. For example, in the Taihangshan–Yanshan region, Yan *et al.*[49] documented a gradual upward trend in FVC (0.02/10 years) from 2000 to 2021, characterized by spatial heterogeneity primarily influenced by evapotranspiration and surface temperature. This aligns with our findings of significant positive correlations with precipitation ($r > 0.6$) and negative correlations with temperature ($r < -0.5$) in grasslands and farmlands, underscoring the pronounced climatic influence on vegetation dynamics. Similarly, Qiao *et al.*[50] identified a fluctuating upward FVC trend (0.26%/year) from 2000 to 2023 in the Qilian Mountains, exhibiting nonlinear responses to

temperature (a biphasic hump-shaped pattern with a threshold at 0°C) and precipitation (diminishing marginal effects with thresholds at 300 mm and 450 mm). These patterns align with our observed 1–2-month precipitation lag and topographic constraints, resulting in local anti-persistence (Hurst index of 0.44) in desert and mountainous areas. In the Yellow River Basin of Henan Province, Shi *et al.*[51] reported a substantial FVC enhancement (67.7%) from 1990 to 2020, with elevation as the dominant driver (q = 0.3) and strong coupling with precipitation, consistent with our results on elevation-induced spatial heterogeneity and climate-topography interactions. Liu *et al.*[52] observed FVC increases across 90.64% of the Jinghe River Basin area from 1998 to 2019, with significant correlations to the precipitation concentration index (18.47%), supporting our identification of precipitation's notable role in vegetation recovery. Furthermore, Tian *et al.*[53] in the Yangtze River Delta described post-2016 FVC fluctuations (initial decline followed by growth), predominantly driven by climate variables with spatial modulation by elevation and slope, which validates our post-2000 increase, post-2010 stabilization, and regional persistence based on the Hurst index (0.81). These congruences affirm that in arid regions, FVC improvements are primarily climate-mediated, with topographic factors exacerbating spatial variations and thresholds governing nonlinear responses.

The short-term forecasting results based on regression models indicate that FVC in the study area will remain relatively stable, with a slight upward trend, during 2024–2028, resulting in an overall increase of approximately 0.01 over the next 5 years. A closer look at the beginning of the forecast period reveals that in 2024, the linear and quadratic models predict FVC values of 0.232 and 0.227, respectively, which increase slightly in 2025 to 0.235 and 0.229, respectively. These narrow and consistent confidence intervals highlight the robustness of the forecasts, suggesting that no abrupt changes in vegetation are expected in the near term. Such stability aligns with the relatively steady patterns observed over the past two decades. It should be emphasized that these forecasts are derived from a univariate annual time series model and thus primarily represent an extrapolation of historical trends rather than a mechanistic explanation of vegetation dynamics. Consequently, the results are best interpreted as short-term, forward-looking references. Future studies could expand on this work by incorporating additional environmental or ecological drivers, such as climate variability or land-use changes, or by adopting more spatially explicit modeling approaches, to capture potential heterogeneity and provide more targeted insights for ecological management and policy-making.

This study relies on MODIS NDVI (250 m resolution) and 1 km climate data, which may overlook micro-scale fluctuations. Future research should integrate Landsat imagery and field measurements to better assess the impacts of high-temperature anomalies and combine socioeconomic data to explore policy implications. Moreover, clustering approaches based on vegetation types or climatic zones could be applied to identify regions with similar FVC dynamics,[54,55] estimate the relative contributions of climatic and anthropogenic drivers, and improve forecasting accuracy through regression or hybrid models. Such methods have been successfully applied in other scientific domains, demonstrating their potential to deepen the analysis of influencing factors in ecological studies.

Shache and Bachu counties need to protect their water resources to sustain grassland recovery, while Zepu and Tumushuke counties should promote the cultivation of drought-tolerant species. Yecheng and Shache counties should optimize irrigation management, and Zepu and Bachu counties should implement afforestation on bare land. Climate adaptation strategies, such as oasis expansion, are critical, and future monitoring should focus on temperature thresholds and precipitation fluctuation.

In view of the potential uncertainties associated with the application of large-scale remote sensing data, future research will strengthen the deployment of ground-based sampling sites and integrate them with multidimensional remote sensing information to establish a more refined data calibration framework. Moreover, the potential errors of the methods used in this study should be acknowledged. For example, the accuracy of the pixel dichotomy approach depends on the selection of NDVI thresholds, which may lead to underestimation or overestimation of FVC in heterogeneous landscapes. In contrast, Hurst analysis assumes time-series stationarity and may be sensitive to noise and short-term fluctuations, potentially biasing persistence estimates. Similarly, the Sen+Mann–Kendall tests, though widely applied, have been critically assessed by Serinaldi *et al*.,[56] who highlighted their mathematical inconsistencies and limitations under certain conditions, such as sample size and serial correlation. Future research may consider improved procedures, such as the Hamed[57] correction, to better account for long-term persistence. These limitations should be taken into account when interpreting the results. Simultaneously, machine learning methods can

be employed to optimize feature extraction and model fitting of remote sensing data, thereby enabling it to more closely approximate ground-based observations across spatial and temporal scales.

This study primarily examined the spatiotemporal variation characteristics of FVC and its correlation with climatic factors in the Yarkand River Basin from 2000 to 2023. Future research should further integrate anthropogenic indicators, such as population density, industrial development, and socioeconomic activities, to better capture the human footprint on FVC. In addition, time series decomposition methods could be applied to separate seasonal components from long-term trends, which would help reveal intra-annual fluctuations in vegetation dynamics and provide a more refined understanding of temporal variation patterns.

5. Conclusion

In summary, this study integrated MODIS NDVI data and climate observations from 2000 to 2023, utilizing pixel dichotomy modeling, Sen+Mann–Kendall trend analysis, and Pearson correlation to examine the spatiotemporal dynamics and climatic drivers of FVC in the Yarkand River Basin. The key findings are as follows:

(i) Significant spatial heterogeneity: FVC exhibited pronounced spatial variability across the Yarkand River Basin, with agricultural land and forests showing high coverage (51.75% and 60.81% medium-high to high coverage, respectively) compared to bare land's low coverage (95.58%). Yecheng County exhibited higher FVC (33.80% high coverage) compared to Bachu County (79.80% low coverage), primarily due to its favorable topography and irrigation practices. These county-level and land-use-specific patterns provided critical insights into spatially targeted ecological restoration in arid environments.

(ii) Temporal trends and stabilization: FVC increased significantly from 0.16 to 0.22 since 2000, stabilizing at 0.21–0.23 post-2010, with grasslands and croplands showing substantial growth (grassland FVC: 0.26 to 0.40; farmland FVC: 0.67 to 0.77). Bare land FVC remained low (0.03 to 0.06), indicating limited ecological recovery. This trend, supported by oasis expansion and water management, highlighted the efficacy of human interventions in enhancing FVC.

(iii) Persistence dynamics: The Hurst index analysis of the long-term time series revealed strong positive persistence (Hurst coefficient = 0.81), driven by oasis agriculture and ecological restoration, ensuring sustained FVC stability across the region. This positive persistence underscored the long-term effectiveness of environmental management in maintaining FVC, particularly in oasis areas, while highlighting the need for continued conservation efforts to address vulnerabilities in desert and mountainous zones.

(iv) Climatic influences: Temperature negatively impacted crop land and forest FVC (highly significant negative correlation: 21.97% for farmland, 20.45% for forests), especially in Zepu County (39.44% negative correlation), due to enhanced evapotranspiration. Precipitation positively drove grassland and forest FVC (highly significant positive correlation: 47.91% for grasslands, 46.75% for forests), with a 1–2-month lag effect notably in Shache and Yecheng Counties (positive correlation: ~60%). The regional temperature rise (from 8.4°C to 9.4°C) and precipitation increase (from 35 mm to 49 mm) aligned with FVC improvements, emphasizing the climate's critical role.

(v) Practical implications and scientific contributions: These findings provided actionable insights for ecological conservation and sustainable water resource management in arid regions. The high FVC stability in oasis areas (e.g., Tumushuke City, slope = 0.009, R^2 = 0.819) supported scaling irrigation and afforestation policies, while bare land's high volatility (74.51%) called for drought-tolerant species and windbreak plantations.

For climate adaptation, Shache and Yecheng Counties should optimize water allocation, while Bachu and Makit Counties require enhanced afforestation. The study's long-term (2000–2023) multi-scale analysis and novel findings, such as the precipitation lag effect and strong regional persistence, advanced the understanding of vegetation-climate interactions, offering a replicable framework for arid ecosystem research globally (e.g., supporting Sustainable Development Goal 13: Climate Action).

Acknowledgments

None.

Funding

This work was supported by the Sub-project of the Major Science and Technology Special Project of

Xinjiang Uygur Autonomous Region, China (Grant Number 2023A02012-1-3), titled "Research on the System for Optimal Allocation of Water Resources at the Watershed Scale."

Conflict of interest

The authors declare that they have no conflicts of interest. The funders had no role in the design of the study; in the collection, analysis, or interpretation of data; in the writing of the manuscript; or in the decision to publish the results.

Author contributions

Conceptualization: Guoqiang Qin, Kai Yuan, Guoliang Ding
Formal analysis: Guoqiang Qin, Kai Yuan
Investigation: Guoqiang Qin, Kai Yuan, Qiang Guo, Runbo Wang
Methodology: Guoqiang Qin, Kai Yuan
Writing–original draft: Guoqiang Qin, Kai Yuan
Writing–review & editing: Guoqiang Qin, Guoliang Ding

Availability of data

This study utilized datasets that are publicly available from the following sources:

(i) Meteorological data were obtained from the National Meteorological Information Center - China Meteorological Data Service Center (http://data.cma.cn).
(ii) Geospatial and environmental data were acquired from the National Earth System Science Data Center (http://www.geodata.cn).
(iii) Remote sensing data products were sourced from NASA Earth Data (https://earthdata.nasa.gov).
(iv) Data processing and analysis were conducted using the GEE platform (https://earthengine.google.com).

All data supporting the findings of this study are available from the aforementioned public repositories.

References

1. Tucker CJ, Pinzon JE, Brown ME, *et al*. An extended AVHRR 8-km NDVI dataset compatible with MODIS and SPOT vegetation NDVI data. *Int J Remote Sens*. 2005;26(20):4485-4498. doi: 10.1080/01431160500168686
2. Fensholt R, Langanke T, Rasmussen K, *et al*. Greenness in semi-arid areas across the globe 1981–2007 - an Earth Observing Satellite based analysis of trends and drivers. *Remote Sens Environ*. 2012;121:144-158. doi: 10.1016/j.rse.2012.01.017
3. Piao S, Wang X, Park T, *et al*. Characteristics, drivers and feedbacks of global greening. *Nat Rev Earth Environ*. 2019;1(1):14-27. doi: 10.1038/s43017-019-0001-x
4. Xu M, Wu H, Kang S, Chen X, Wang Y. Climate change decreased the effect of meltwater on cotton production in the Yarkant river basin of arid northwest China. *Irrig Sci*. 2024;42(1):99-114. doi: 10.1007/s00271-023-00862-x
5. Zhan C, Liang C, Zhao L, *et al.* Vegetation dynamics and its response to climate change in the yellow river Basin, China. *Front Environ Sci*. 2022;10:892747. doi: 10.3389/fenvs.2022.892747
6. Komissarov A, Komissarov M, Safin K, Ishbulatov M, Kovshov Y. Long-term irrigation effect on soil and vegetation cover of floodplain estuaries in the Southern Urals. *Asian J Water Environ Pollut*. 2020;17(1):83-90. doi: 10.3233/AJW200009
7. Chen Y, Li Z, Fan Y, Wang H, Deng H. Progress and prospects of climate change impacts on hydrology in the arid region of northwest China. *Environ Res*. 2015;139:11-19. doi: 10.1016/j.envres.2014.12.029
8. Li Z, Chen Y, Li W, Deng H, Fang G. Potential impacts of climate change on vegetation dynamics in Central Asia. *JGR Atmos*. 2015;120(24):12345-12356. doi: 10.1002/2015JD023618
9. Lioubimtseva E, Cole R, Adams JM, Kapustin G. Impacts of climate and land-cover changes in arid lands of Central Asia. *J Arid Environ*. 2005;62(2):285-308. doi: 10.1016/j.jaridenv.2004.11.005
10. Xiao J, Jin Z, Wang J. Assessment of the hydrogeochemistry and groundwater quality of the Tarim river basin in an extreme arid region, NW China. *Environ Manag*. 2014;53(1):135-146. doi: 10.1007/s00267-013-0198-2
11. Deng H, Chen Y, Wang H, Zhang S. Climate change with elevation and its potential impact on water resources in the Tianshan Mountains, Central Asia. *Global Planet Change*. 2015;135:28-37. doi: 10.1016/j.gloplacha.2015.09.015
12. Chen Z, Chen Y, Li B. Quantifying the effects of climate variability and human activities on runoff for Kaidu River Basin in arid region of northwest China. *Theor Appl Climatol*. 2013;111(3-4):537-545. doi: 10.1007/s00704-012-0680-4
13. Zhang Q, Gu X, Singh VP, Shi P, Sun P. More frequent flooding? Changes in flood frequency in the Pearl River basin, China, since 1951 and over the past 1000 years. *Hydrol Earth Syst Sci*. 2018;22(5):2637-2653. doi: 10.5194/hess-22-2637-2018
14. Amuti T, Luo G. Analysis of land cover change and its

driving forces in a desert oasis landscape of Xinjiang, northwest China. *Solid Earth*. 2014;5(2):1071-1085. doi: 10.5194/se-5-1071-2014
15. Zhao Y, Cao B, Sha L, *et al*. Land use and cover change and influencing factor analysis in the Shiyang River Basin, China. *J Arid Land*. 2024;16(2):246-265. doi: 10.1007/s40333-024-0071-6
16. Xu J, Chen Y, Li W, Nie Q, Hong Y, Yang Y. The nonlinear hydro-climatic process in the Yarkand River, northwestern China. *Stoch Environ Res Risk Assess*. 2013;27(2):389-399. doi: 10.1007/s00477-012-0606-9
17. Bhambri R, Bolch T, Chaujar RK, Kulshreshtha SC. Glacier changes in the Garhwal Himalaya, India, from 1968 to 2006 based on remote sensing. *J Glaciol*. 2011;57(203):543-556. doi: 10.3189/002214311796905604
18. Fu A, Li W, Wang Y, Bai Y. Basic and target eco-environment water requirements of a dry inland river under typical flow frequencies in China. *PeerJ*. 2020;8:e8285. doi: 10.7717/peerj.8285
19. Hou Y, Chen Y, Ding J, Li Z, Li Y, Sun F. Ecological impacts of land use change in the arid Tarim river Basin of China. *Remote Sens*. 2022;14(8):1894. doi: 10.3390/rs14081894
20. Yi Y, Liu S, Zhu Y, Wu K, Xie F, Saifullah M. Spatiotemporal heterogeneity of snow cover in the central and western Karakoram Mountains based on a refined MODIS product during 2002–2018. *Atmos Res*. 2021;250:105402. doi: 10.1016/j.atmosres.2020.105402
21. Sulla-Menashe D, Friedl MA. *User Guide to Collection 6 MODIS Land Cover (MCD12Q1 and MCD12C1) Product.* Available from: https://lpdaac.usgs.gov/documents/101/MCD12_User_Guide_V6.pdf [Last accessed on 2025 Apr 13]. doi: 10.5067/MODIS/MCD12Q1.006
22. Gorelick N, Hancher M, Dixon M, Ilyushchenko S, Thau D, Moore R. Google earth engine: Planetary-scale geospatial analysis for everyone. *Remote Sens Environ*. 2017;202:18-27. doi: 10.1016/j.rse.2017.06.031
23. Kaur A, Ghosh S, Das SK. Satellite image-based land use/land cover dynamics and forest cover change analysis (1996-2016) in Odisha, India. *Asian J Water Environ Pollut*. 2019;16(1):25-39. doi: 10.3233/AJW190004
24. Li F, Chen W, Zeng Y, Zhao Q, Wu B. Improving estimates of grassland fractional vegetation cover based on a pixel dichotomy model: A case study in inner Mongolia, China. *Remote Sens*. 2014;6(6):4705-4722. doi: 10.3390/rs6064705
25. Jiapaer G, Chen X, Bao A. A comparison of methods for estimating fractional vegetation cover in arid regions. *Agric Forest Meteorol*. 2011;151(12):1698-1710. doi: 10.1016/j.agrformet.2011.07.004
26. Shi S, Yu J, Wang F, Wang P, Zhang Y, Jin K. Quantitative contributions of climate change and human activities to vegetation changes over multiple time scales on the Loess Plateau. *Sci Total Environ*. 2021;755:142419. doi: 10.1016/j.scitotenv.2020.142419
27. Li X, Liu Y, Wang L. Change in fractional vegetation cover and its prediction during the growing season based on machine learning in southwest China. *Remote Sens*. 2024;16(19):3623. doi: 10.3390/rs16193623
28. Fu B, Yang W, Yao H, *et al*. Evaluation of spatio-temporal variations of FVC and its relationship with climate change using GEE and Landsat images in Ganjiang River Basin. *Geocarto Int*. 2022;37(26):13658-13688. doi: 10.1080/10106049.2022.2082551
29. Zeng B, Wen B, Zhang X, *et al*. Analysis on spatiotemporal variation in soil drought and its influencing factors in Hebei province from 2001 to 2020. *Agriculture*. 2025;15(10):1109. doi: 10.3390/agriculture15101109
30. Yang R, Li X, Mao D, Wang Z, Tian Y, Dong Y. Examining fractional vegetation cover dynamics in response to climate from 1982 to 2015 in the Amur River Basin for SDG 13. *Sustainability*. 2020;12(14):5866. doi: 10.3390/su12145866
31. Mao L, Pei X, He C, *et al*. Spatiotemporal changes in vegetation cover and soil moisture in the lower reaches of the Heihe river under climate change. *Forests*. 2024;15(11):1921. doi: 10.3390/f15111921
32. Huang J, Li Y, Fu C, *et al*. Dryland climate change: Recent progress and challenges. *Rev Geophys*. 2017;55(3):719-778. doi: 10.1002/2016RG000550
33. Yao T, Bolch T, Chen D, *et al*. The imbalance of the Asian water tower. *Nat Rev Earth Environ*. 2022;3(10):618-632. doi: 10.1038/s43017-022-00299-4
34. Immerzeel WW, Lutz AF, Andrade M, *et al*. Importance and vulnerability of the world's water towers. *Nature*. 2020;577(7790):364-369. doi: 10.1038/s41586-019-1822-y
35. Duveiller G, Hooker J, Cescatti A. The mark of vegetation change on Earth's surface energy balance. *Nat Commun*. 2018;9(1):679. doi: 10.1038/s41467-017-02810-8
36. Zhu Z, Piao S, Myneni RB, *et al*. Greening of the Earth and its drivers. *Nat Clim Change*. 2016;6(8):791-795. doi: 10.1038/nclimate3004
37. Zhou Q, Chen W, Wang H, Wang D. Spatiotemporal evolution and driving factors analysis of fractional vegetation coverage in the arid region of northwest China. *Sci Total Environ*. 2024;954:176271. doi: 10.1016/j.scitotenv.2024.176271

38. Zhang K, Kimball JS, Nemani RR, Running SW. A continuous satellite-derived global record of land surface evapotranspiration from 1983 to 2006. *Water Resour Res*. 2010;46(9):2009WR008800.
doi: 10.1029/2009WR008800
39. Deng Y, Wang X, Wang K, *et al*. Responses of vegetation greenness and carbon cycle to extreme droughts in China. *Agric Forest Meteorol*. 2021;298-299:108307.
doi: 10.1016/j.agrformet.2020.108307
40. Vicente-Serrano SM, Gouveia C, Camarero JJ, *et al.* Response of vegetation to drought time-scales across global land biomes. *Proc Natl Acad Sci USA*. 2013;110(1):52-57.
doi: 10.1073/pnas.1207068110
41. Dimitriadis P, Koutsoyiannis D. Climacogram versus autocovariance and power spectrum in stochastic modelling for Markovian and Hurst–Kolmogorov processes. *Stoch Environ Res Risk Assess*. 2015;29(6):1649-1669.
doi: 10.1007/s00477-015-1023-7
42. Dimitriadis P, Koutsoyiannis D, Iliopoulou T, Papanicolaou P. A Global-scale investigation of stochastic similarities in marginal distribution and dependence structure of key hydrological-cycle processes. *Hydrology*. 2021;8(2):59.
doi: 10.3390/hydrology8020059
43. Wei S, Li X, Wang K, Wang T, Piao S. Two decades of persistent greening in China despite 2023 climate extremes. *Sci China Earth Sci*. 2025;68(4):1064-1073.
doi: 10.1007/s11430-024-1530-7
44. Cao S, Zhang L, He Y, *et al*. Effects and contributions of meteorological drought on agricultural drought under different climatic zones and vegetation types in Northwest China. *Sci Total Environ*. 2022;821:153270.
doi: 10.1016/j.scitotenv.2022.153270
45. Wang H, Guan H, Liu B, Chen X. Impacts of climate extremes on vegetation dynamics in a transect along the Hu Line of China. *Ecol Indic*. 2023;155:111043.
doi: 10.1016/j.ecolind.2023.111043
46. Qi X, Jia J, Liu H, Lin Z. Relative importance of climate change and human activities for vegetation changes on China's silk road economic belt over multiple timescales. *CATENA*. 2019;180:224-237.
doi: 10.1016/j.catena.2019.04.027
47. Urban MC, Alberti M, De Meester L, *et al*. Interactions between climate change and urbanization will shape the future of biodiversity. *Nat Clim Chang*. 2024;14(5):436-447.
doi: 10.1038/s41558-024-01996-2
48. Gao X, Wen R, Lo K, Li J, Yan A. Heterogeneity and non-linearity of ecosystem responses to climate change in the Qilian Mountains National Park, China. *J Arid Land*. 2023;15(5):508-522.
doi: 10.1007/s40333-023-0101-9
49. Yan F, Guo X, Zhang Y, *et al*. Analysis of the multiple drivers of vegetation cover evolution in the Taihangshan-Yanshan region. *Sci Rep.* 2024;14(1):15306.
doi: 10.1038/s41598-024-66053-6
50. Qiao B, Cao X, Yang H, *et al*. Nonlinear threshold effects of environmental drivers on vegetation cover in mountain ecosystems: From constraint mechanisms to adaptive management. *Ecol Indic*. 2025;173:113328.
doi: 10.1016/j.ecolind.2025.113328
51. Shi S, Wang X, Hu Z, *et al*. Geographic detector-based quantitative assessment enhances attribution analysis of climate and topography factors to vegetation variation for spatial heterogeneity and coupling. *Glob Ecol Conserv*. 2023;42:e02398.
doi: 10.1016/j.gecco.2023.e02398
52. Liu Y, Huang T, Qiu Z, Guan Z, Ma X. Effects of precipitation changes on fractional vegetation cover in the Jinghe River basin from 1998 to 2019. *Ecol Inform*. 2024;80:102505.
doi: 10.1016/j.ecoinf.2024.102505
53. Tian X, Tao Z, Xie Y, Shao W, Zhang S. Spatiotemporal evolution and driving mechanism of fractional vegetation coverage in the Yangtze river delta. *IEEE J Sel Top Appl Earth Observ Remote Sens*. 2024;17:10979-10997.
doi: 10.1109/JSTARS.2024.3407727
54. Marincowitz S, Pham NQ, Wingfield BD, Roets F, Wingfield MJ. Microfungi associated with dying *Euphorbia mauritanica* in South Africa and their relative pathogenicity. *Fungal Syst Evol.* 2023;12(1):59-72.
doi: 10.3114/fuse.2023.12.04
55. Litvinenko V. *Advances in Raw Material Industries for Sustainable Development Goals*. 1st ed. Boca Raton: CRC Press; 2020.
doi: 10.1201/9781003164395
56. Serinaldi F, Chebana F, Kilsby CG. Dissecting innovative trend analysis. *Stoch Environ Res Risk Assess*. 2020;34(5):733-754.
doi: 10.1007/s00477-020-01797-x
57. Hamed KH. Trend detection in hydrologic data: The Mann-Kendall trend test under the scaling hypothesis. *J Hydrol*. 2008;349(3-4):350-363.
doi: 10.1016/j.jhydrol.2007.11.009